A Comparison of NiMo/γ-Al₂O₃ Catalysts Prepared by Impregnation and Coprecipitation for Dibenzothiophene Hydrodesulfurization: Kinetic Study

Fang Liu [a], Tinghua Guo [b], Xiaoguang Wang [c]

Department of Chemistry, Zhoukou Normal University, Zhoukou 466001, China

[a]liu_fang11@sina.com.cn, [b]13623521658@139.com, [c]wangqinghua201@163.com

Abstract

A comparison of NiMo/γ- Al₂O₃ catalysts prepared by impregnation and coprecipitation was conducted with x-ray diffraction (XRD) analysis and tested for dibenzothiophene (DBT) hydrodesulfurization (HDS). XRD observed the appearance of γ- Al₂O, and NiAl₂O₄ over impregnation NiMo/γ- Al₂O and γ- Al₂O, MoO₃, β-NiMoO₄ over coprecipitation NiMo/γ- Al₂O₃. The formation of β-NiMoO₄ from MoO₃ and NiO in the coprecipitation NiMo/γ- Al₂O is attributed to higher DBT HDS activity than impregnation NiMo/γ- Al₂O. Both pseudo- first-order kinetic model and simplified Langmuir–Hinshelwood (L-H) model were examined with experimental data. The pseudo-first-order kinetic model fitted better with data and appeared more applicable than simplified L-H model. The activation energies for DBT HDS over impregnation and coprecipitation catalysts are 83 kJ/mol·K and 34 kJ/mol·K from pseudo-first-o rder kinetic model and 110 kJ/mol·K and 73 kJ/mol·K from simplified L-H model, respectively. Both models gave lower activation energy on the coprecipitation catalyst than the impregnation catalyst, which explains the observed higher HDS activity from the coprecipitation catalyst over the impregnation catalyst from a kinetics perspective.

Keywords

NiMo/Al₂O₃, hydrodesulfurization, coprecipitation, impregnation, kinetics.

1. Introduction

The hydrodesulfurization (HDS) remains one of the key processes to produce clean and ultra clean transportation fuel in an effort of meeting progressively stringent environmental regulations.[1-3] The use of conventional hydrotreating catalysts in complex and integrated refineries for deep desulfurization would require severe operating conditions such as high temperature and low space velocity to reach an allowed low level of sulfur content. Such severe processing conditions generally lead to rapid catalyst deactivation, shorter cycle times, reduced throughput, and increased energy consumption.[4] Catalysts are the heart of many commercial chemical processes and material phase composition is one of the critical parameters determining the catalyst performance. Therefore, learning the catalyst phase composition and understanding the chemical reaction kinetics are necessary to commercialize the high efficient and cost-effective HDS process.[5]

In numerous HDS kinetic studies,[6-8] either the pseudo-first-order kinetic model, Langmuir–Hinshelwood (L-H) model or both was used with the dibenzothiophene (DBT) as one of the representative model compounds. The HDS of DBT has been overwhelmingly reported to occur as pseudo-first-order with respect to DBT regardless of the catalysts used and experimental conditions.[6,7] Considering the fact that HDS of DBT is a heterogeneous catalysis process, the L-H model has also been extensively studied to combine the effect of adsorption, surface reaction, desorption, and active sites on the reaction kinetics.[8]

In our previous work,[3] we reported that a NiMo/γ-Al₂O₃ catalyst prepared by coprecipitation exhibited much higher activity for DBT HDS than that prepared by impregnation. The objectives of

this study are to determine the catalyst material phase composition to further reveal the active sites and to learn the reaction kinetics by using pseudo-first-order kinetic model and L-H model.

2. Experimental

2.1 Reagents and catalysts

Reagents used in this work included DBT (98% purity, Sigma-Aldrich), carbon disulfide (98% purity, Xilong Chemical Factory), decahydronaphthalene (98% purity, Sinopharm Chemical Reagent Co. Ltd.), cyclohexylbenzene (99.5% purity, Shengqi Chemical Factory), and biphenyl (99.5% purity, Jinmaotai Chemical Factory). All the reagents were used without further purification. Two catalysts prepared by impregnation and coprecipitation methods were provided by Luknova Inc, without sulfidation. Impregnation catalyst was prepared by incipient wetness impregnation of the γ-Al$_2$O$_3$ support with aqueous solutions of molybdenum trioxide and nickel nitrate.[9, 10] Aqueous ammonia was added into the solution of molybdenum trioxide and nickel nitrate under stirring conditions until the metal precursors were completely dissolved. The mixed solution was used to impregnate the γ-Al$_2$O$_3$ support (surface area 180 m^2/g, Alfa Aesar) at room temperature. After an overnight drying at room temperature, the resultant sample was further dried at 393 K for 12 h in air and then was calcined at 673 K for 2 hours. The obtained catalyst sample was denoted as catalyst-impregnation, NiMo/Al$_2$O$_3$ consisting of 16.5% Mo and 4.4% Ni. Catalyst-coprecipitation was prepared by the coprecipitation method in aqueous media by homogenously mixing aluminum oxide precursor with molybdenum trioxide and nickel nitrate. The metal loading of the coprecipitation catalyst was nearly the same as impregnation catalyst.

2.2 Apparatus and procedure

The experimental apparatus and procedure were reported elsewhere.[3] A trickled-bed reactor of i.d.10 mm stainless steel tube was used to evaluate the catalyst activity by feeding 1.0 wt % dibenzothiophene in decahydronaphthalene. The reactor was packed from bottom to top in three sections. The bottom and top sections were packed with 40-60 mesh SiC and the center section was loaded with 2 mL mixture of 40-60 mesh catalyst sample and 40-60 mesh SiC at 1:1 weight ratio. The experimental apparatus mainly consisted of a high pressure feed pump, a stainless steel tubular reactor, an electric furnace, a temperature controller and indicator, a gas-liquid separator, and flow meters. A thermal couple was placed in the middle of the catalyst bed to monitor reaction temperature. The intraparticle and interphase mass transfer limitations were found to be negligible in this study. Prior to the feed introduction, the catalyst was presulfided with 3-vol% carbon disulfide (CS$_2$) in decahydronaphthalene. A standard presulfidation procedure includes following steps: (1) purging the reactor with hydrogen for 30 mins at room temperature and 3.0 MPa pressure; (2) increasing the reactor temperature from room temperature to 150 ºC in 30 mins; (3) maintaining the temperature at 150 ºC for 10 mins; (4) introducing H$_2$ at 47 mL/min and presulfidation feed of 3% CS$_2$ in decahydronaphthalene at 0.095 mL/min at 150 ºC and then increasing the reactor temperature from 150 to 300 ºC in 30 mins; and (5) maintaining the presulfidation of the step (4) at 300 ºC for 5 hours. After the presulfidation, the catalyst activity for hydrodesulfurization was evaluated by lowering the reaction temperature to the target temperatures and then feeding 1 wt % dibenzothiophene (DBT) in decahydronaphthalene into the reactor. Within the tested conditions, there are no observable catalyst deactivation and hydrocracking of the solvent decahydronaphthalene.

2.3 Analysis

The liquid products collected from a gas-liquid separator were analyzed by off-line gas chromatograph equipped with a flame ionization detector and an OV-1701 (50 m $\times$ 0.25 mm $\times$ 0.5μm) capillary column. The column, injection, and detector temperatures were set at 250 ºC, 280 ºC, and 280 ºC, respectively. Main hydrodesulfurization products were cyclohexylbenzene and biphenyl. Each component in liquid products was identified and quantified by using standard compounds. The catalyst performance in terms of total conversion and the product selectivity was found stable after 4 hours of on-stream testing. Typically, the catalyst was tested for 7 hours to generate steady-state data

in this work. X-Ray Diffraction (XRD) data were collected using CuKα radiation and a Rigaku Miniflex diffractometer from 10 to 90º 2θ with a step-width of 0.02º. BET surface area and pore size measure were conducted using a Micromeritics ASAP 2010 instrument.

3. Results and Discussion

3.1 XRD Analysis

Figure1 illustrates the XRD profiles of three samples prepared by impregnation method and calcined at 673K, coprecipitation method and calcined at 673K, and coprecipitation method without calcination. The characteristic indices of γ-Al_2O_3 were observed as two sharp peaks at 2θ of 46º and 67º, as well as broad bands at 2θ of 36º and 62º. The absence of Ni or Mo-related indices on impregnation catalyst suggests that two metal oxides are dispersed on Al_2O_3 in amorphous phase or microcrystallines. As compared with impregnation catalyst, the prominent XRD features for coprecipitation catalysts are the appearance of MoO_3 and β-$NiMoO_4$ over calcined coprecipitation catalyst and mainly MoO_3 over uncalcined coprecipitation catalyst. The formation of β-$NiMoO_4$ indicates the solid state reaction occurred possibly between MoO_3 and amorphous phase or microcrystallines NiO at 673K.
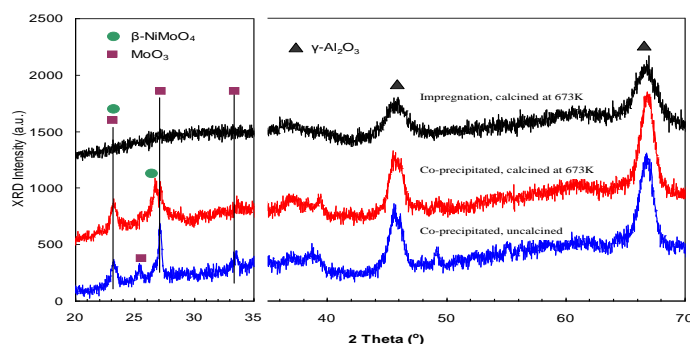

Figure 1. XRD patterns of NiMo/γ-Al_2O_3 catalysts prepared by impregnation calcined at 673K, coprecipitation and calcined at 673K, and coprecipitation without calcination.

3.2 DBT conversion at various LHSVs

Figure 2 presents the steady-state DBT conversion as a function of liquid hourly space velocity (LHSV) over NiMo/γ-Al_2O_3 catalysts prepared by impregnation and coprecipitation at various temperatures. At the same temperature, the DBT conversions over both catalysts decreased with increasing LHSV, most likely due to reduced residence time. At the same LHSV, the catalyst prepared by coprecipitation exhibited higher DBT conversion than the catalyst prepared by impregnation. Lower LHSV is always preferable for both catalysts to reach high conversions, but the catalyst prepared by coprecipitation exhibited a significant potential of processing more feedstock over that prepared by impregnation. Since 1-wt% DBT feed was used in this study, the effect of H_2S formation and its competitive adsorption for active sites on the overall reaction rate is negligible.
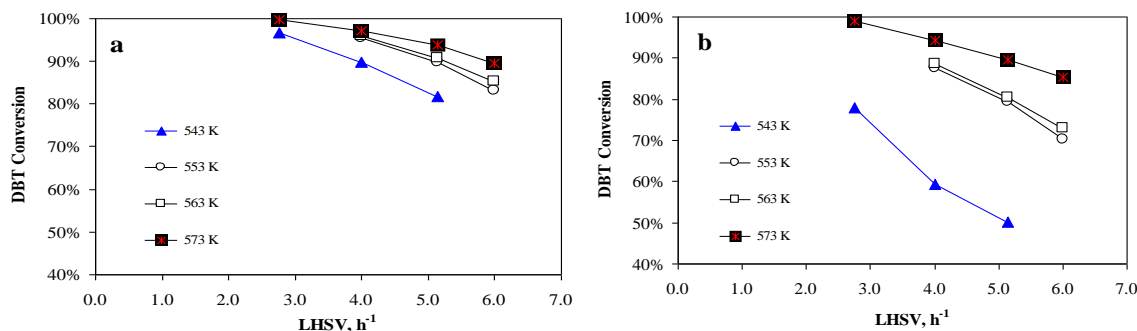

Figure 2. The steady-state DBT conversion as a function of liquid hourly space velocity (LHSV) over NiMo/γ-Al_2O_3 catalysts prepared by (a) coprecipitation and (b) impregnation **at** various temperatures.

3.3 Kinetics of DBT HDS

The pseudo-first-order kinetic model and Langmuir–Hinshelwood model have been extensively used to reveal the difference in the intrinsic properties of the different HDS catalysts, such as activation energy. The NiMo/γ-Al$_2$O$_3$ catalysts prepared by impregnation and coprecipitation were tested and the experimental data were analyzed using the pseudo-first-order model and Langmuir–Hinshelwood model, respectively.

3.4 Pseudo-first-order kinetic model

The simple pseudo-first-order kinetic model was frequently used to fit kinetic data and obtain kinetic parameters in HDS of DBT and its derivatives. It is assumed the reactor operates under isothermal and plug flow conditions. The integrated rate equation of the pseudo-first-order model for a plug-flow reactor is as follows

$$-\ln(1-x) = \frac{k_{HDS}}{LHSV} \tag{1}$$

Where x is the DBT conversion, k_{HDS} is the apparent rate constant, and $LHSV$ is the liquid hourly space velocity, respectively. Figure 3 shows the $-\ln(1-x)$ plot against $\frac{1}{LHSV}$ at various temperatures over NiMo/γ-Al$_2$O$_3$ catalysts prepared by impregnation and coprecipitation. The straight lines as shown in Figures 4a and 4b all passed through the origin within the tested conditions. The results indicated that the experimental data is well fitted into the pseudo-first-order model for DBT HDS over both studied catalysts. According to Arrhenius equation, the rate constant can be expressed as

$$k_{HDS} = A_0 Exp\left(\frac{-E}{RT}\right) \tag{2}$$

$$-\ln\left(k_{HDS}\right) = -\ln\left(A_0\right) + \frac{E}{RT} \tag{3}$$

Where A_0 is the Arrhenius constant; E is the activation energy, kJ/mol; R is gas constant, kJ/mol·K; and T is temperature, K. Figure 5 illustrates the Arrhenius plot of $-\ln(k_{HDS})$ versus $1/T$ for both catalysts. The apparent rate constants and activation energies were calculated from the slopes and intercepts of both straight lines as shown in Figure 5. The calculated activation energies for DBT HDS over catalysts prepared by impregnation and coprecipitation are 83 kJ/mol·K and 34 kJ/mol·K, respectively. The activation energy for DBT HDS over coprecipitation catalyst is significantly lower than that over impregnation catalyst, which explains well why the coprecipitation catalyst exhibited higher activity than impregnation catalyst. The activation energies and Arrhenius constants obtained from simple pseudo-first-order kinetic model are further compared with those obtained from Langmuir–Hinshelwood model in Table 2.
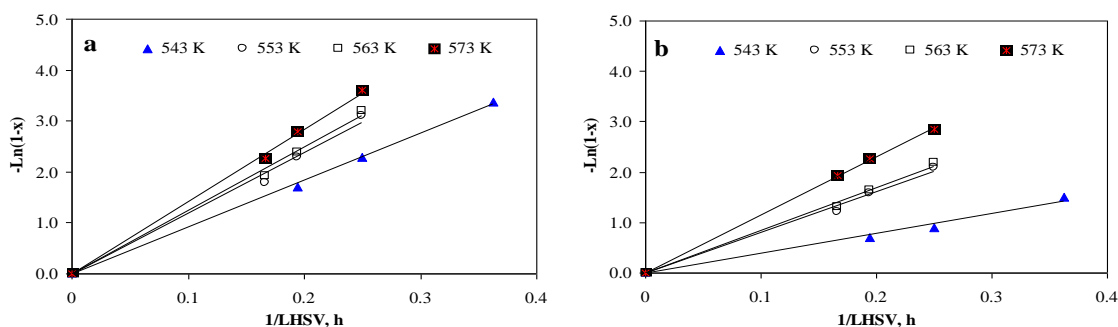

Figure 3. The $-Ln(1-x)$ plots against 1/LHSV at various temperatures over NiMo/γ-Al$_2$O$_3$ catalysts prepared by (a) coprecipitation and (b) impregnation.

3.3.1 Langmuir–Hinshelwood model

In the kinetic studies of HDS reactions of dibenzothiophenic compounds, the Langmuir-Hinshelwood (L-H) model was extensively used due to the consideration of fundamental steps of surface reactions, including adsorption, surface reaction, and desorption. Catalyst properties, such as active site number, and reaction conditions affect or even determine the conversion and product selectivity significantly. The catalyst properties, such as surface area, surface coverage, and the number of active site, may gradually change with prolonged test, but we assumed that all the physical and chemical properties are either almost the same or the changes do not cause significant effect on the catalyst performance in this study. Except the desired reaction conditions changes, it is assumed that the reaction temperature, pressure, and species concentrations are constant through the entire catalyst bed.
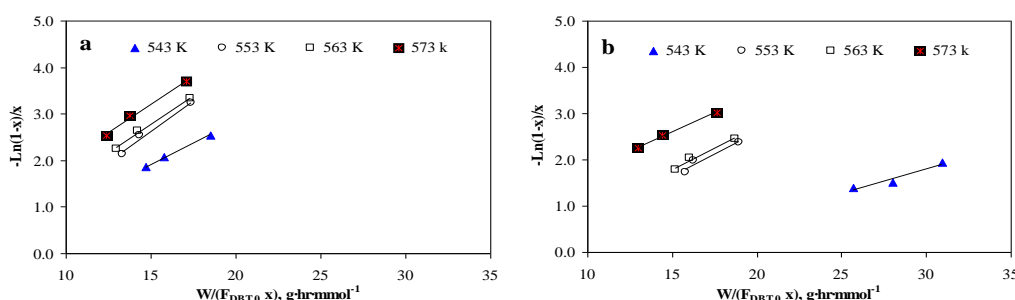

Figure 4. The plots of $-Ln(1-x)/x$ against $W/(F_{DBT,0}x)$ at various temperatures over NiMo/γ-Al$_2$O$_3$ catalysts prepared by (a) coprecipitation and (b) impregnation.

The dual-site L-H model has been aggressively accepted to reveal the reaction kinetics of the DBT HDS reaction: one site for DBT and its products competitive adsorption and the other site for H$_2$ adsorption. Therefore, the following dual-site L-H equation is used in this approach:

$$\gamma_{HDS} = \frac{k'_{HDS} K_{DBT} K_{H_2} P_{DBT} P_{H_2}}{(1 + K_{DBT} P_{DBT} + K_{H_2S} P_{H_2S})(1 + K_{H_2} P_{H_2})} \tag{4}$$

where γ_{HDS} is the rate of HDS reaction; k'_{HDS} is the rate constant of HDS reaction; K_{DBT}, K_{H_2S}, and K_{H_2} are the adsorption equilibrium constants of DBT, H$_2$S, and H$_2$, respectively; and P_{DBT}, P_{H_2S}, and P_{H_2} are the partial pressures of DBT, H$_2$S, and H$_2$, respectively. Within the tested conditions the H$_2$ pressure was constant and H$_2$S formation was negligible due to the low DBT concentration (1.0-wt %) under a high H$_2$ pressure (3.0 MPa). Therefore, the Eq. (4) can be simplified into Eqs. (5) and (6):

$$\gamma_{HDS} = \frac{k'_{HDS} K_{DBT} P_{DBT}}{(1 + K_{DBT} P_{DBT})} \tag{5}$$

$$\frac{1}{r_{HDS}} = \frac{1}{k'_{HDS} K_{DBT} P_{DBT}} + \frac{1}{k'_{HDS}} \tag{6}$$

The DBT can be treated as an ideal gas and then its partial pressure can be written as:

$$P_{DBT} = C_{DBT,0}(1-x)RT \tag{7}$$

where $C_{DBT,0}$ is the molar concentration of DBT in the feed; x is the DBT conversion; R is the gas constant, and T is the reaction temperature. Then the equation (6) can be further integrated and simplified to give following rate expression for a plug flow reactor:

$$-\frac{\ln(1-x)}{x} = k'_{HDS} K_{DBT} C_{DBT,0} \times \left(\frac{W}{F_{DBT,0}x} \right) - K_{DBT} C_{DBT,0} \tag{8}$$

where W is catalyst weight and $F_{DBT,0}$ is the molar flow rate of DBT. Figure 4 shows the plots of $-\dfrac{\ln(1-x)}{x}$ against $\dfrac{W}{F_{DBT,0}x}$ at various temperatures. The straight lines in Figure 5 indicated that the experimental data are well fitted into the simplified L-H model. By plotting $-\dfrac{\ln(1-x)}{x}$ against $\dfrac{W}{F_{DBT,0}x}$, the k'_{HDS} and K_{DBT} can be calculated by determination of the relevant slope and intercept with the y axis. Figure 6 depicts the Arrhenius plot of $-\ln(k'_{HDS})$ versus $1/T$ for both catalysts based on L-H model. According to the slopes and intercepts of both straight lines as shown in Figure 7, the calculated activation energies for DBT HDS over catalysts prepared by impregnation and coprecipitation are 110 kJ/mol·K and 73 kJ/mol·K, respectively. The activation energy for DBT HDS over coprecipitation catalyst is also significantly lower than that over impregnation catalyst.
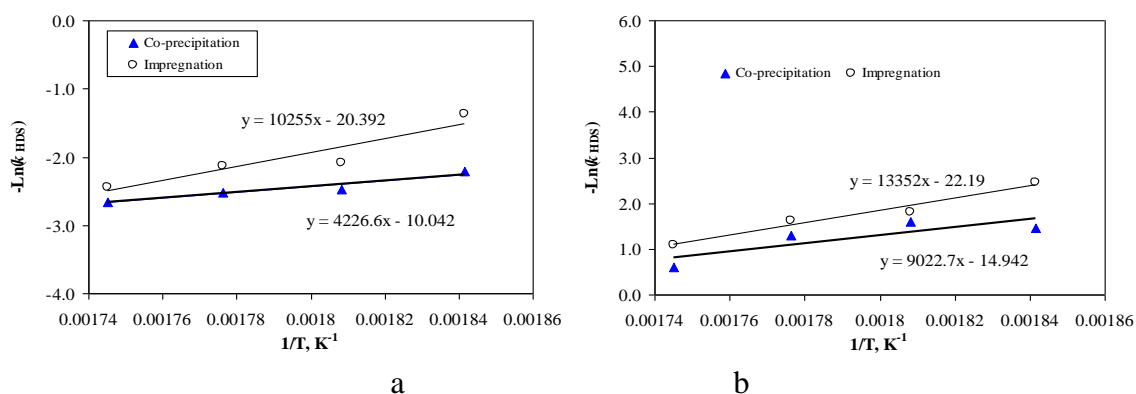

Figure 5. Arrhenius plot of $-Ln(k'_{HDS})$ versus $1/T$ for DBT HDS over NiMo/γ-Al$_2$O$_3$ catalysts prepared by coprecipitation and impregnation methods based on simplified Langmuir–Hinshelwood (L-H) model(a) and pseudo-first-order kinetic model(b).

3.3.2 Comparison of Pseudo-first-order model and Langmuir–Hinshelwood model

Table 1 compared the apparent rate constants and activation energies obtained from pseudo-first-order model and simplified L-H model. Both activation energies and Arrhenius constants calculated from pseudo-first-order model are lower than those from simplified L-H model. This may be due to the fact that the presence of DBT adsorption and two active sites reaction mechanism were considered in the simplified L-H model. A few of HDS studies reported that L–H model led to higher activation energies and Arrhenius constants than power law model due to the presence of competitive adsorption between reactant and products.[11]

Table 1. The apparent rate constants and activation energies obtained from pseudo-first-order model and simplified L-H **model**

	Pseudo-first-order		Langmuir–Hinshelwood	
	E^a, kJ/mol·K	A_0^b	E^a, kJ/mol·K	A_0^b
NiMo/γ-Al$_2$O$_3$ prepared by impregnation	83	7.18×10^8	110	4.34×10^9
NiMo/γ-Al$_2$O$_3$ prepared by coprecipitation	34	2.30×10^4	73	3.08×10^6

a-Activation energy; b-Arrhenius constant.

Both pseudo-first-order model and simplified L-H model gave lower activation energy over the coprecipitation catalyst than the impregnation catalyst. This explains the observed higher HDS activity from the coprecipitation catalyst over the impregnation catalyst from the perspective of chemical kinetics.

4. Conclusion

NiMo/γ-Al$_2$O$_3$ catalysts prepared by impregnation and coprecipitation were compared by using X-ray diffraction (XRD) technique and DBT HDS reaction. XRD observed the appearance of γ-Al$_2$O$_3$, and NiAl$_2$O$_4$ over impregnation NiMo/γ-Al$_2$O$_3$ and γ-Al$_2$O$_3$, MoO$_3$, β-NiMoO$_4$ over coprecipitation NiMo/γ-Al$_2$O$_3$. The formation of β-NiMoO$_4$ from MoO$_3$ and NiO in the coprecipitation NiMo/γ-Al$_2$O$_3$ is attributed to higher DBT HDS activity than impregnation NiMo/γ-Al$_2$O$_3$. Both pseudo-first-order kinetic model and simplified Langmuir–Hinshelwood (L-H) model were examined with experimental data to reveal kinetics. The pseudo-first-order kinetic model fitted better with experimental data and appeared more applicable than simplified L-H model. Both models give lower activation energy over the coprecipitation catalyst than the impregnation catalyst, which explains the observed higher HDS activity from the coprecipitation catalyst over the impregnation catalyst from a kinetic perspective.

Acknowledgements

References

[1] Ramos RR, Bolívar C, Castillo J, Hung J, Scott CE. Ultrasound assisted synthesis of nanometric Ni, Co, NiMo and CoMo HDS catalysts. *Catal Today.* 2008;133-135: 277-281.

[2] Oyama ST, Gott T, Zhao H, Lee YK. Transition metal phosphide hydroprocessing catalysts: A review. *Catal Today.* 2009;143:94-107.

[3] Liu F, Xu S, Cao L, Chi Y, Zhang T, Xue D. A comparison of NiMo/Al$_2$O$_3$ catalysts prepared by impregnation and coprecipitation methods for hydrodesulfurization of dibenzothiophene. *J Phys Chem C.* 2007;111:7396-7402

[4] Stockle M, Knight T. Impact of low-sulphur bunkers on refineries. PTQ Catalysis, 2009; 14:27-31.

[5] Leliveld B, Mayo S. Increasing ULSD production with current assets. PTQ Catalysis 2009;14:51-54.

[6] Wang Y, Sun Z, Wang A, Ruan L, Lu M, Ren J, Li X, Li C, Hu Y, Yao P. Kinetics of hydrodesulfurization of dibenzothiophene catalyzed by sulfided Co-Mo/MCM-41. *Ind Eng Chem Res.* 2004;43:2324-2329.

[7] Farag H, Whitehurst DD, Sakanishi K, Mochida I, Improving kinetic analysis of sequential and parallel reactions of hydrodesulfurization of dibenzothiophenes by establishing reasonable boundaries for reaction rate constants. *Catal Today.* 1998;50:49-56.

[8] kagami N, Vogelaar BM, Van Langeveld AD, Moulijn JA. Reaction pathways on NiMo/Al$_2$O$_3$ catalysts for hydrodesulfurization of diesel fuel. *Appl Catal A: Gen.* 2005;293:11-23.

[9] Laredo GC, Córtes CM. Kinetics of hydrodesulfurization of dimethyldibenzothiophenes in a gas oil narrow-cut fraction and solvent effects. Appl Catal A: Gen. 2003;252:295-304.

[10] Katsuhisa F, Masafumi S, Tetsuro K. (Nippon Ketjen Co., Ltd.; Akzo Nobel N.V.). Hydroprocessing catalyst and process. U.S. Patent 6,656,349, December 2, 2003.

[11]   Katsuhisa F, Tetsuro K, Masafumi S, Yoshimasa I. (Nippon Ketjen Co., Ltd.). Hydroprocessing catalyst and use thereof. U.S. Patent 5,888,380, March 30, 1999.

[12]   Ferdous D, Dalai AK, Adjaye J. Hydrodenitrogenation and hydrodesulfurization of heavy gas oil using NiMo/Al$_2$O$_3$ catalyst containing boron: experimental and kinetic studies. *Ind Eng Chem Res*. 2006;45:544-552.